CONTROL MODELS OF SWITCH MODE MAXIMUM POWER POINT TRACKING INTERFACES FOR ENERGY HARVESTING DEVICES

Tzern T. Toh, Paul D. Mitcheson, Eric M. Yeatman
Department of Electrical & Electronic Engineering, Imperial College London, United Kingdom
tzern.toh@imperial.ac.uk

Abstract: In this paper, we present a method to model and control the interface electronics in order to obtain maximum power transfer from a rotational energy harvester. A state-space representation of a boost converter (with component parasitics) was derived and embedded in a control loop that performs input impedance matching to the armature resistance of the rotational harvester. Root locus techniques were used to choose the proportional-integral (PI) controller gain. A comparison of simulation results from Matlab and PSpice are presented. The methods reported in this paper are valid for other types of harvesters and interface electronics by changing the modelling parameters. It was found that increasing the controller gains results in a more damped closed-loop system response and for this specific example, the closed-loop behaviour is non-oscillatory for all positive values of gain.

Keywords: rotational energy harvester, maximum power point tracking, control of power electronics

INTRODUCTION

Energy harvesting devices present a novel and integrated solution to battery-less wireless sensor nodes. The power levels obtainable from an energy harvester usually vary in the μW to mW range, depending on the type of harvester used. For this reason, there is a fundamental requirement to transfer maximum power from the harvester to the electrical load in order to realise a completely self-powered system. Generally, this necessitates some form of impedance match between the transducer and the electrical load, *i.e.* control of the input impedance of the power electronics that interface the transducer.

We have previously reported experimental results from a single-attachment-point rotational energy harvester (Fig. 1) interfaced to an optimized, self-starting maximum power point tracker (MPPT) enabled sensor-node, operating as a wireless shaft-encoder [1]. In this paper, state-space averaged control model development, root-locus analysis and controller design for the MPPT switch-mode power electronic interface is presented, allowing control gains to be chosen and system stability to be investigated. We believe this is the first time that such techniques have been applied to miniature energy harvesting devices.

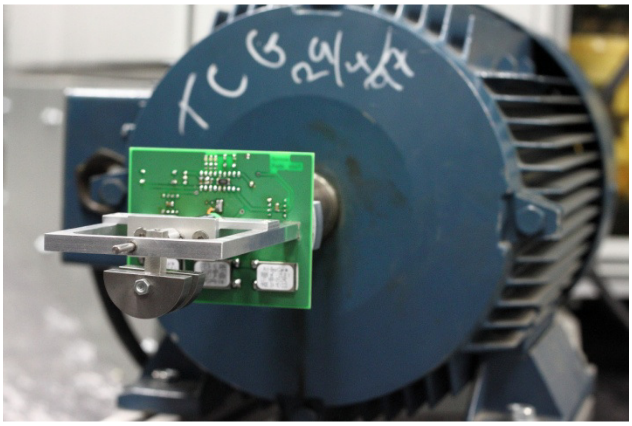

Fig. 1: Experimental setup of the rotational energy harvester mounted onto an induction machine.

CONTROL MODELS OF THE MAXIMUM POWER POINT TRACKING INTERFACE

A boost converter (Fig. 2) performs an impedance match to the generator through modification of the converter's duty cycle, δ. This must be continuously adjusted as the voltage on the storage capacitor and the speed of rotation change. A small-signal state-space averaged model relating generator EMF (E_G) to the inductor current was formulated using techniques in [2]. These have previously been applied to controller design for output regulation of switch-mode power supplies [3] in the presence of a disturbance. However, the models presented in [3] are not applicable here because the controller was used for output voltage regulation, hence a new model was derived.

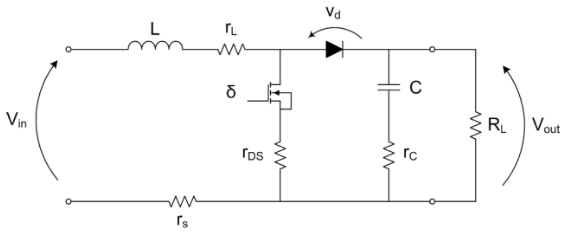

Fig. 2: Schematic of a boost converter with its parasitic terms: r_L and r_C are the series resistances of the inductor and capacitor, r_{DS} is the on-resistance of the MOSFET and r_s is a sense resistor used to measure the inductor current.

State-Space Model of a Boost Converter

A state-space model of the boost converter with predefined input and output vectors was constructed in Matlab. Three input variables were fed into the model; the boost converter's input voltage, diode voltage drop, and the duty cycle, as shown in Fig. 3. In order to test the boost converter model in isolation, the converter's input voltage, V_{in}, was represented by an external reference input that undergoes a step change, and the effects of this change were observed in the inductor current. At this juncture, it was assumed that the inductor current was continuous.

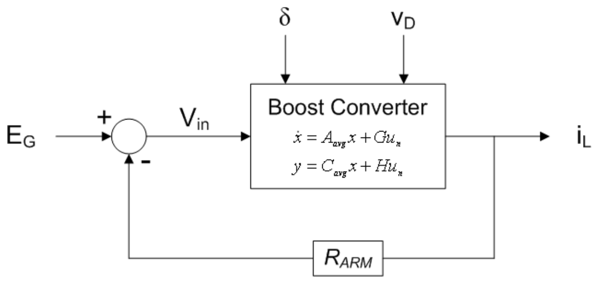

Fig. 3: Connections made to the boost converter state-space model in Matlab to analyse the closed loop step response of i_L when E_G changes.

The closed-loop transfer function of this system is given by (1).

$$\frac{i_L}{E_G} = \frac{s\left(\frac{1}{L}\right) + \frac{1}{LC(r_C + R_L)}}{\left[s^2 + s\alpha + \beta\right] + R_{ARM}\left[s\left(\frac{1}{L}\right) + \frac{1}{LC(r_C + R_L)}\right]} \quad (1)$$

where

$$\alpha = \frac{1}{C(r_C + R_L)} + \frac{1}{L}\left(r_L + r_s + \delta r_{DS} + (1-\delta)\frac{r_C R_L}{r_C + R_L}\right)$$

$$\beta = \frac{1}{LC(r_C + R_L)} + \left[r_L + r_s + \delta r_{DS} + \frac{(1-\delta) r_C R_L}{r_C + R_L} + \frac{(1-\delta)^2 R_L^2}{r_C + R_L}\right]$$

State-Space Model Verification

This model was compared with a large signal time-domain simulation in PSpice (Fig. 4), to verify the inductor current waveform when the reference input, E_G, undergoes a step change, representing a change in the rotational energy harvester's speed. The simulation parameters for both models are listed in Table 1.

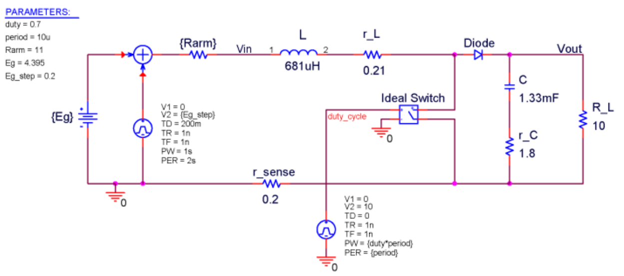

Fig. 4: PSpice circuit used to verify the Matlab transfer function, i_L/E_G, with a step input on E_G.

Table 1: Simulation parameters for the model in Fig. 4

Parameter	Value
Initial E_G	4.3 V
E_G step change	0.2 V
Duty cycle	0.7

The circuit was simulated for 400 ms and the value of E_G was fixed until 200 ms, at which point a step increase of 0.2 V was applied to the initial value of E_G. All other variables were held constant throughout the simulation. The averaged inductor current from Matlab and PSpice is shown in Fig. 5.

As can be seen, there is good agreement between the circuit simulation model and the state-space model from Matlab (the averaged inductor currents differ by less than 1 mA). This constant offset does imply that there is a slight discrepancy between the two models which could be caused by the diode voltage being modelled as a constant in Matlab, whereas PSpice models the full diode I-V characteristics. As far as PSpice is concerned, the Matlab state-space model is accurate.

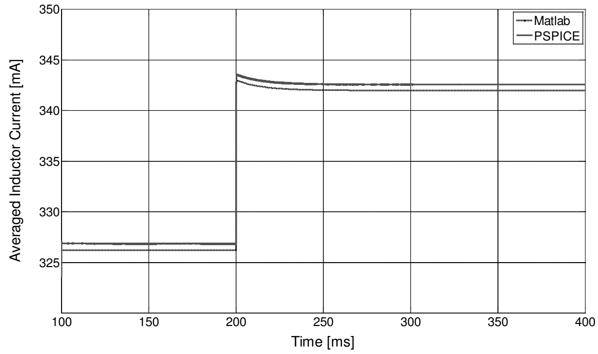

Fig. 5: Step response comparison of the averaged inductor current waveforms from Matlab and PSpice.

The waveforms from Matlab do not have switching ripples because the state-space averaging method used to derive the models does not include this information. Closer inspection of the instantaneous inductor current from PSpice, as depicted in Fig. 6, shows that the switching ripples are evident, with a peak-to-peak value of 6.6 mA, which is considerably smaller than its averaged value. This validates the prior assumption that the converter was operating in continuous conduction.

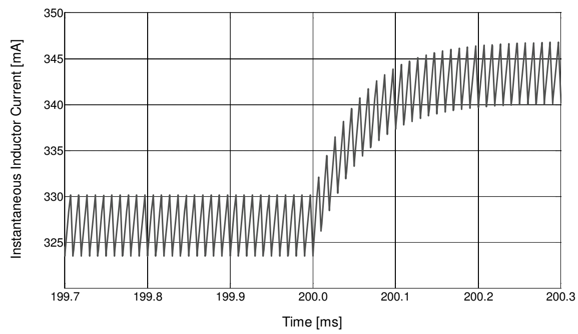

Fig. 6: Switching ripples in the instantaneous inductor current in PSpice.

Closed-Loop Model of the Input Impedance Matching Circuit

Having verified the transfer function in Eq. (1), a Matlab model of the impedance matching circuitry was constructed and this included a proportional-integral (PI) controller with the boost converter plant model in the complete closed loop system (Fig. 7).

Due to the complexity of this model, the Matlab function `connect` was used to specifically connect the blocks as shown in the figure. Each block consists of either a transfer function or state-space model that defines its input to output behaviour. The objective now is to obtain a transfer function that relates E_G to i_L, in this closed-loop configuration as a function of controller gains. The difference between the measured and demand currents was passed through a forward gain, K, followed by the PI-controller, which then generates the duty cycle which will eventually reduce the error. In this simulation, the PI-controller gains (K_p and K_i) were set prior to building the closed-loop model shown in Fig. 7. Therefore, changing K will effectively scale both K_p and K_i proportionally.

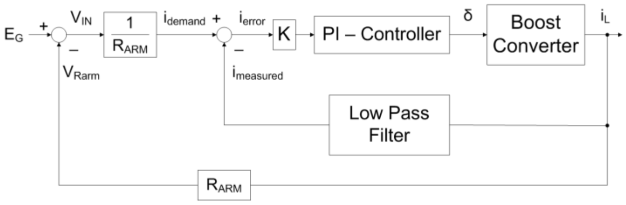

Fig. 7: Closed-loop Matlab model of the impedance matching circuitry used to investigate the circuit response to changes in the generated voltage, E_G.

In PSpice, the input impedance controller was implemented using the Analog Behavioural Modelling (ABM) library, as shown in Fig. 8. This model was used to validate the functionality of the Matlab model in Fig. 7. The only difference between the two closed-loop models is the existence of the PWM signal generator in the PSpice model. In Matlab, all that is required by the boost converter's state-space model is the numerical value of the duty cycle.

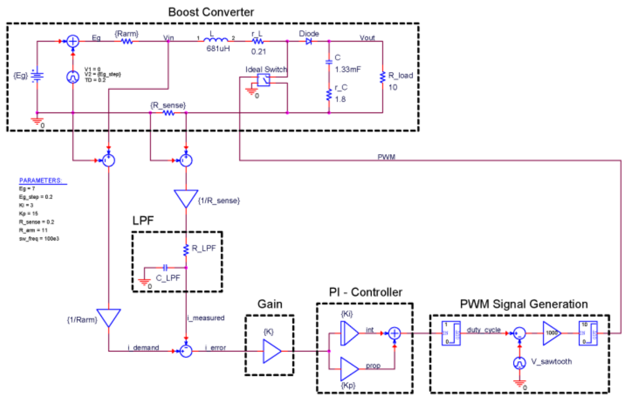

Fig. 8: Closed-loop PSpice model of the experimental circuit that implements the input impedance match.

The circuit was simulated for 280 ms and the step increase in E_G (0.2 V) occurs at 200 ms. All the circuit components are identical to the simulation conducted for the schematic in Fig. 4, and the initial choice of controller gains were 3 and 15 for K_p and K_i respectively. The PI-controller gains for the interface circuit that was built and experimentally tested in [1] were chosen by inspection, based on the amount of jitter present in the PWM gate drive signal and response time of the controller. Once the Matlab model was verified with the simulation results from PSpice, the root locus plots of the closed-loop transfer function were inspected to determine improved and substantiated PI-controller gains.

The behaviour of the averaged inductor current from both models is plotted in Fig. 9. There is a good agreement between the small and large-signal closed-loop models for a simulated step change in generator speed. Unlike the previous model, where it was possible to calculate the steady state value of the inductor current prior to the step change, the equations governing the closed-loop model were iteratively obtained because a closed form solution is not possible.

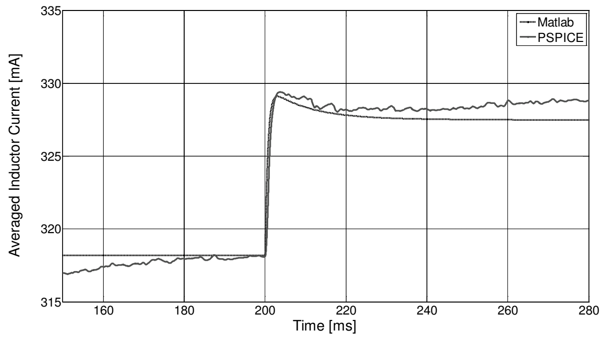

Fig. 9: Comparison of the averaged inductor current waveforms from Matlab and PSpice for the closed-loop input impedance matching circuit model.

Intuitively, if the generated voltage remains constant for a long period of time, the inductor current should settle to a value of $E_G/2R_{ARM}$, assuming that the PI-controller gains are suitably chosen. For the simulation results shown in Fig. 9, E_G was set to 7 V and thus, the steady state inductor current should settle at about 318 mA, prior to the step change, as is seen.

ROOT LOCUS ANALYSIS

Having verified the Matlab closed-loop model (Fig. 7), the root locus plots of the system can now be investigated. In such a plot, the behaviour of the system's closed-loop poles can be visually analysed when a system parameter is changed (usually the system's forward control loop gain).

The transfer function for the closed-loop model with the embedded switch mode converter shown in Fig. 7 is:

$$\frac{i_L(s)}{E_G(s)} = \frac{2.49\times10^{-7}s^3 + 2.68\times10^{-4}s^2 + 0.02s + 0.09}{s^4 + 1.86\times10^4 s^3 + 1.88\times10^7 s^2 + 1.18\times10^9 s + 1.97} \quad (2)$$

Eq. (2) gives three real zeros at -996, -75, -5 and four real poles at -1.75×10^4, -1000, -68, 0, all of which are in the left half plane, on the real axis. A plot of the root locus (with increasing values of forward gain) for the aforementioned poles and zeros is given in Fig. 10, and Fig. 11 shows the area around the origin of the same root locus. This plot was obtained using the Single-Input-Single-Output Design Tool in Matlab.

As the forward gain, K, was increased from zero to a large value (typically known as infinite gain), the closed-loop poles were observed to move further along the negative real axis with no imaginary parts. The damping factor, ζ, is given by $\cos(\alpha)=\zeta$ where α is the angle that the root locus makes with respect to the real axis. For all positive values of K, this closed-loop system has a damping factor of 1. In fact, the system behaviour will be more damped (and stable) as K is increased because the closed-loop poles will be located further along the negative real axis. Note that this stability is specific to component values in the circuit presented in [1], and Eq. (2) may contain complex poles and zeros for different circuit component values.

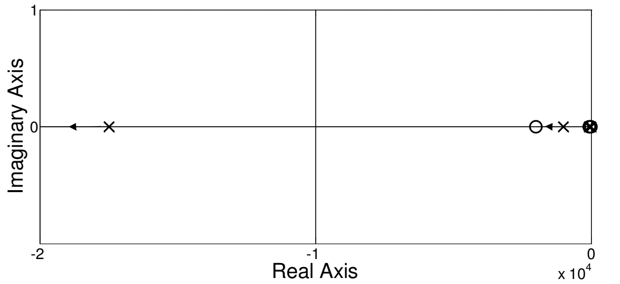

Fig. 10: Root locus plot of the transfer function i_L/E_G for the Matlab model in Fig. 7.

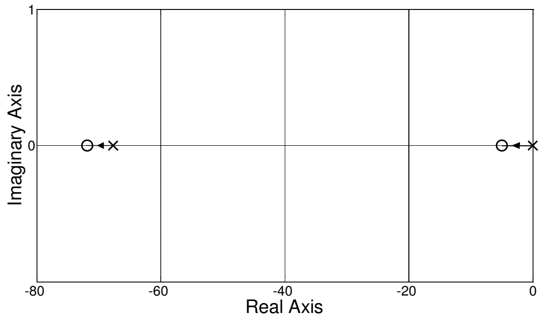

Fig. 11: Root loci near the origin.

A comparison between the closed-loop system responses from Matlab and PSpice is plotted in Fig. 12 for a 0.2 V step increase in the generated voltage, E_G. For different values of forward gain, the averaged inductor currents are plotted on the left column and the input impedance on the right. In both cases, the time domain simulation lasted 180 ms with the step change occurring at 90 ms. Prior to the step change, the averaged inductor current reached a steady state value of 318 mA for E_G = 7 V and R_{ARM} = 11 Ω.

The plots in Fig. 12 indicate a strong agreement between the two models with discrepancies of less than 5 mA for the gain values. With increasing values of K, it is evident that the input impedance settles more quickly at the target value of 11 Ω for both models. When K = 1, the averaged inductor current does not reach the steady state value before the step change in E_G. This indicates that there is insufficient proportional and integral gain to reduce the error between the demand and measured currents.

CONCLUSIONS

Using classical control design, we have developed and verified a power electronics interface controller for an energy harvesting device. The results presented in this paper can be expanded to include other types of harvesters or interface circuitry. In the present implementation, higher PI-gain values will result in a more stable and damped system. Future developments of the control models will include the potential mechanical instability of the rotational energy harvester if the offset mass flips over and synchronises with the rotation source. In addition to that, PI-controller gain scheduling may be required because the rotational harvester operates under two regimes: matched impedance for maximum power transfer or current limiting to prevent flip over [1].

ACKNOWLEDGEMENTS

This work was supported by the European Community's Seventh Framework Program under grant agreement No. 223975, Project MOBESENS.

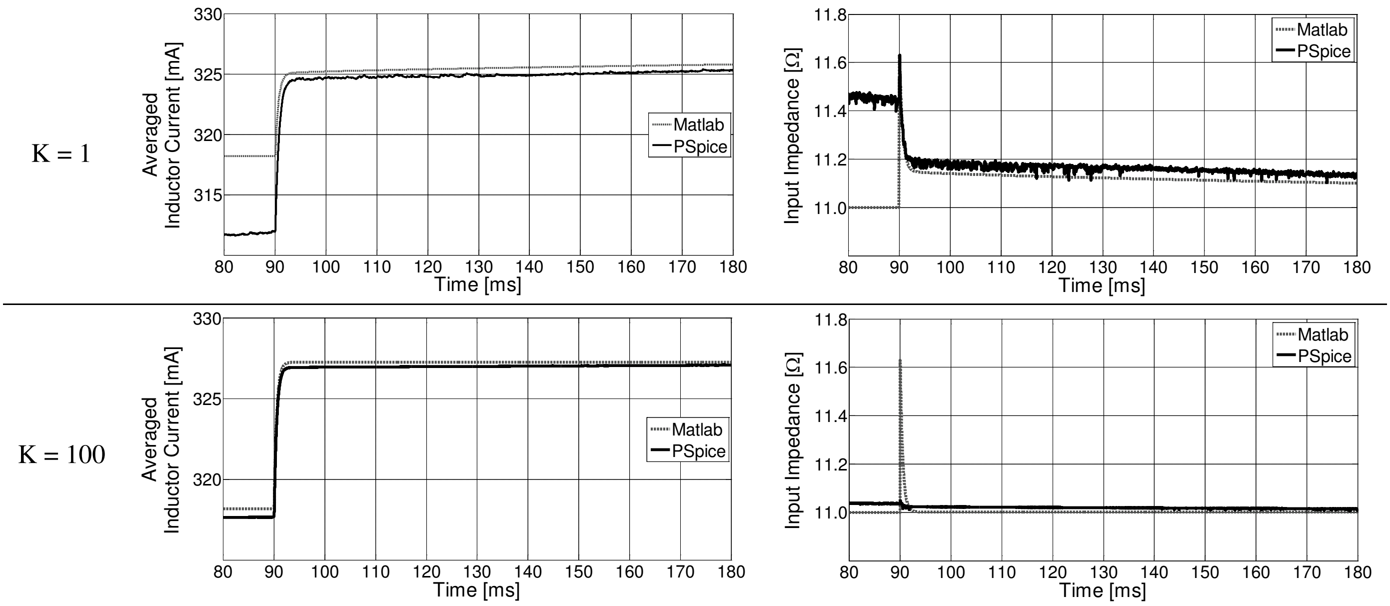

Fig. 12: Step responses of the closed-loop system for forward gains of 1 and 100.

REFERENCES

[1] T. T. Toh, P. D. Mitcheson and E. M. Yeatman, "Wireless Sensor Node Using a Rotational Energy Harvester with Adaptive Power Conversion", in *Proc. PowerMEMS 2009*, pp. 273-276

[2] F. Dong Tan and R. D. Middlebrook, "A Unified Model for Current-Programmed Converters", in *IEEE Trans. Power Electronics*, 10 (1995), pp. 397-408

[3] N. Mohan 1995 *Power Electronics: Converters, Applications and Design* (John Wiley & Sons)